In Situ Thermal Battery Discharge Using CoS_2 as a Cathode Material

Julia L. Payne,[1,z] Julia D. Percival,[2] Kyriakos Giagloglou,[1] Christina J. Crouch,[1,2] George M. Carins,[1] Ronald I. Smith,[3] Richard K. B. Gover,[2] and John T. S. Irvine[1,*]

[1] *School of Chemistry, University of St Andrews, St Andrews, Fife KY16 9ST, United Kingdom*
[2] *AWE, Aldermaston, Reading RG7 4PR, United Kingdom*
[3] *ISIS facility, STFC Rutherford Appleton Laboratory, Harwell Campus, Didcot OX11 0QX, United Kingdom*

Thermal batteries are an established primary battery technology and the most commonly used cathodes in these batteries are transition metal disulfides MS_2 (where M = Co, Ni and Fe). However, understanding the evolution of crystalline phases upon battery discharge has been hindered due to the high temperature operation of these batteries. Here we report an experiment that simultaneously collects powder neutron diffraction and electrochemical data as the battery is discharged. Four regions are observed in the diffraction data and four different cobalt containing phases are observed. Multi-phase Rietveld refinement has been used to monitor the evolution of phases during discharge and this is linked to the battery discharge profile. A new discharge mechanism has been proposed which involves hexagonal CoS instead of Co_3S_4, and the increase in unit cell parameters on discharge suggests the formation of a sulfur deficient solid solution before transformation to Co_9S_8. This behavior seems reminiscent of that of NiS_2 suggesting that the discharge mechanisms of transition metal disulfides may have more similarities than originally thought.
 [DOI: 10.1149/2.1431912jes]

Manuscript submitted March 8, 2019; revised manuscript received July 5, 2019. Published August 2, 2019.

Thermal batteries are an established primary battery technology, which finds use in applications such as emergency power supplies in aircraft. Such applications require a constant power to be drawn over a length of time.

Typically, thermal batteries consist of a cathode, a molten salt electrolyte, separator and anode.[1] A pyrotechnic source is used to heat the battery above the melting point of the electrolyte, which brings about a high ionic conductivity in the electrolyte. The KCl-LiCl eutectic is a common choice of electrolyte, due to its melting point being compatible with the thermal stability of the other battery components and the low solubility of other battery components in the electrolyte.[2] The anode is usually a lithium alloy, such as $Li_{13}Si_4$, which has a high melting point, enabling operation in high temperature batteries.[3] $Li_{13}Si_4$ also possesses a high lithium ion conductivity. MgO is a typical separator and transition metal sulfides are usually used as the cathode.[4]

The most commonly used cathode materials are transition metal disulfides, MS_2 (M = Fe, Co, Ni).[4,5] Although the low cost and natural abundance of FeS_2 favours its use in thermal batteries, there are several advantages of using CoS_2 as a cathode material.[4] These include the higher electronic conductivity, low solubility in the molten salt electrolyte and a higher thermal stability of CoS_2 over FeS_2.[4] CoS_2 is able to provide a higher voltage for longer in comparison to FeS_2, despite the lower voltage of CoS_2 with respect to FeS_2.[4] This is particularly important in applications where thermal batteries are required to provide constant power over extended periods of time.

The optimisation of CoS_2 in thermal battery cathodes is also of interest to help improve performance. CoS_2/carbon nanotube composites have recently been tested and showed an enhanced capacity with respect to CoS_2 whilst retaining good thermal stability.[6] Optimisation of the cathode processing, using spray deposition techniques, has also been studied.[7]

Several phases exist in the Co-S phase diagram.[4] These include CoS_2, Co_3S_4, Co_9S_8 and CoS and these are shown in Figure 1. CoS_2 has the pyrite structure (space group *Pa*-3), which consists of a face centred array of Co atoms, which are surrounded by six sulfur atoms to form slightly distorted corner sharing octahedra. Co_3S_4 has the spinel structure (space group *Fd*-3*m*), which has two cobalt sites, one tetrahedrally coordinated by sulfur and one octahedrally coordinated by sulfur. The NiAs structure is adopted by CoS ($P6_3/mmc$), where cobalt is again at the centre of CoS_6 octahedra. As the sulfur is hexagonally close packed in CoS ($P6_3/mmc$) we can also view the structure with sulfur at the centre of trigonal prisms with Co at the vertices. Co_9S_8 (*Fm*-3*m*) also has cobalt at the centre of octahedra and tetrahedra with sulfur at the vertices. In Co_9S_8, the CoS_6 octahedra are isolated from each other and share corners with the CoS_4 tetrahedra. CoS_4 tetrahedra are linked to each other by their corners and edges.

Several cobalt sulfides, including CoS_2 and Co_9S_8 have also been used as electrodes in room temperature lithium ion batteries.[8–10] A range of synthetic strategies have been probed in an attempt to control the morphology of the cobalt sulfide phases.[9,10] This is of interest as it offers the opportunity to shorten the lithium diffusion pathway and optimize reaction kinetics.[9]

Although the electrochemical properties of transition metal sulfide cathodes MS_2 (M = Ni, Co, Fe) have been studied for many years, the evolution of the crystalline phases during thermal battery discharge has not been probed. This is largely due to the fact that these batteries operate at elevated temperature (~500°C). As a result, experiments to investigate the crystalline phases present during discharge have required stopping the experiment at particular voltages and quenching the sample to room temperature, then collecting diffraction data at room temperature. This can present problems due to the (in)stability of the desired phases at room temperature or phase transitions. We recently reported a combined neutron powder diffraction and battery discharge experiment for a thermal battery which used NiS_2 as a cathode.[11] This study was the first combined in situ diffraction and electrochemical experiment on a thermal battery and provided a new insight into the phase evolution under battery operating conditions.

In situ neutron diffraction has been used to correlate the atomic structure of battery materials with the properties displayed for a number of years and an early example is the study of lithium extraction from the $LiMn_2O_4$ spinel.[12] However, such studies have focused on batteries which operate at room temperature rather than the high temperature battery technologies. Powder neutron diffraction is particularly suitable for studying lithium containing compounds due to lithium's much higher scattering power relative to other atoms (e.g. Co, S) with neutrons compared to X-rays. The use of neutron diffraction in this study is particularly important given the sensitivity to lithium, especially when the differences in discharge mechanisms are considered, as FeS_2 is reported to form lithiated intermediate phases whilst existing reports on CoS_2 suggest that lithiated phases do not form.[13] Therefore the aim of this work is to probe the structure-property relationship in thermal batteries which use a CoS_2 cathode.

*Electrochemical Society Member.
[z]E-mail: jlp8@st-andrews.ac.uk

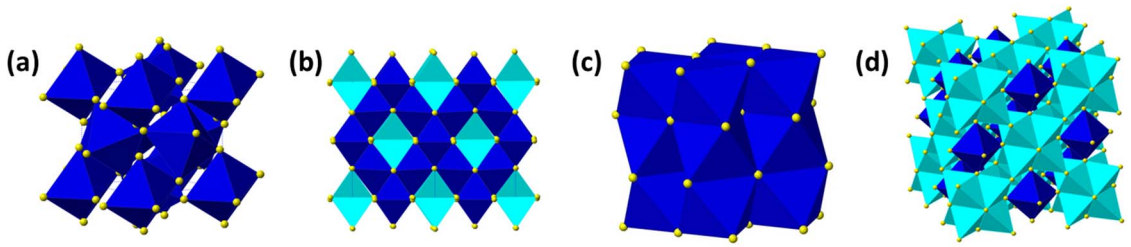

Figure 1. Crystal structures for different cobalt sulfides. (a) CoS_2 with the pyrite structure, (b) Co_3S_4 with the spinel structure, (c) CoS with the NiAs structure and (d) Co_9S_8. Yellow atoms are sulfur, dark blue atoms are cobalt in octahedral sites and light blue is cobalt in tetrahedral sites.

Experimental

Prior to the in situ neutron diffraction experiment, a smaller cell was assembled using CoS_2 (cathode, 0.17 g, 14.0 mmol) as the cathode, $Li_{13}Si_4$ (0.29 g, 14.3 mmol) as the anode, MgO as the separator and the LiCl-KCl eutectic as the electrolyte. The anode, cathode and electrolyte/separator were pressed into pellets separately and then loaded into a Swagelok type assembly in an argon-filled glove box. This enabled electrochemical testing to be carried out ex situ at 520°C in a muffle furnace, using a Maccor battery tester (model 5300). The battery was tested galvanostatically, applying a current density of 127.3 mA cm^{-2}.

Time of flight neutron diffraction data were collected on the Polaris diffractometer at the ISIS neutron source, Rutherford Appleton Laboratory, UK. Polaris is a high intensity medium resolution diffractometer with a large area of detector coverage. Combined, these lead to a very high count rate which lends itself well to the fast data collection required to study battery discharge. The St Andrews Conductivity Rig, which has been specially developed for the simultaneous collection of neutron diffraction and electrochemical data in a controlled atmosphere, which has been described elsewhere, was used for this experiment.[14] The sample holder of the St Andrews Conductivity Rig was adapted for this experiment to use thin vanadium plate as both current collectors for the electrochemical measurements and for holding the sample in place. Vanadium is an excellent choice in this respect, due to its neutron scattering length of −0.38 fm, meaning that the intensities of the Bragg reflections from the sample holder/current collector are very weak, and make negligible contribution to the diffraction pattern compared to the rest of the battery components.

For the neutron diffraction experiment, $Li_{13}Si_4$ (anode, 0.22g, 1.1 mmol), a mixture of LiCl-KCl eutectic (electrolyte), LiBr (separator) and CoS_2 (cathode, 0.64 g, 3.6 mmol) were pressed sequentially into pellets of diameter 23.6 mm and an approximate thickness of 1–2 mm, which were kept under argon until required due to their air and moisture sensitivity. For each neutron diffraction experiment one single cell battery was loaded into the St Andrews Conductivity Rig in an Argon-filled glove box, then the rig was placed in a Rutherford Appleton Laboratory designed furnace which was mounted on the Polaris diffractometer. A Type-K thermocouple was placed inside the rig, approximately 2 cm above the sample holder and was used to control the temperature of the battery during the experiment. All diffraction measurements were carried out under flowing argon due to the air and moisture sensitivity of these samples.

A powder neutron diffraction pattern was collected initially for ∼1 hour at room temperature from the undischarged battery (where the molten salt electrolyte would be solid). Following this, a series of diffraction patterns of 5 minutes duration were collected while the CoS_2 cell was then heated up to 520°C at 10°C/minute in order to monitor any phase changes and confirm melting of the LiCl-KCl eutectic. Following this, the potentiostatic cell discharge was started and over the next ∼18hours a large number of diffraction patterns of 5 minutes duration were collected as the cell discharged. During the discharge, electrochemical data were collected potentiostatically using a Kikusui electrochemical interface.

During the subsequent data reduction, diffraction patterns corresponding to isopotentials in the discharge profile were summed together into single datasets to improve counting statistics and thus allow quantitative phase analysis to be carried out in the Rietveld refinement. Rietveld refinement was carried out using GSAS.[15,16] Film plots of diffraction data were created using the WinPlotr function in Fullprof.[17,18]

Results and Discussion

In order to determine the potentials of interest before the combined in situ neutron diffraction and battery discharge experiment, an ex situ battery discharge experiment was carried out on a CoS_2 cell (with a $Li_{13}Si_4$ anode and a LiCl-KCl eutectic electrolyte). This test was carried out at 520°C, which is sufficiently above the melting point of the KCl-LiCl eutectic for the electrolyte to achieve a high ionic conductivity. The cell was discharged galvanostatically and the resulting battery discharge profile is shown in Figure 2. Figure 2 clearly shows the presence of two regions, one at 1.45 V and one at 1.05 V. This is in agreement with the two plateaux observed at around 1.75-1.6 V and ∼1.13 V when tested with a Li-Si anode and a LiBr-KBr-LiCl eutectic electrolyte at 500°C.[4]

Figure 3 shows the room temperature powder neutron diffraction pattern obtained from the battery before discharge. The broad features in the background are due to the amorphous quartz sample holder. Several phases were identified in the diffraction pattern

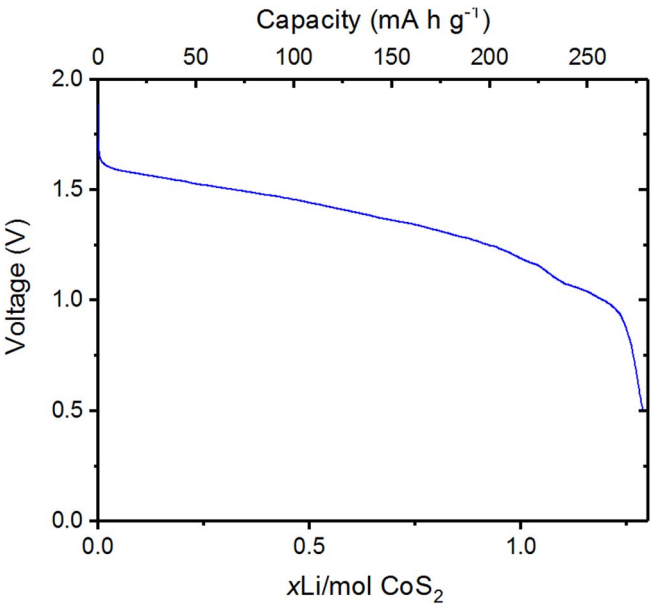

Figure 2. Ex situ battery discharge profile using CoS_2 as a cathode at 520°C and a current density of 127.3 mA cm^{-2}.

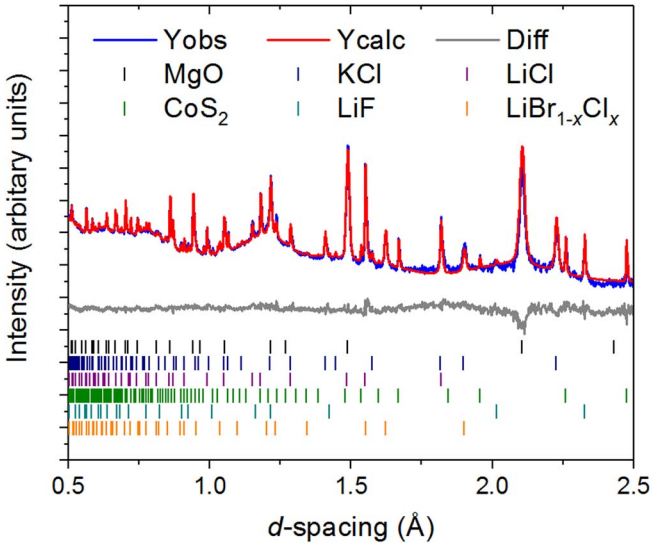

Figure 3. Multiphase Rietveld fit for data collected at room temperature on the CoS_2 cell.

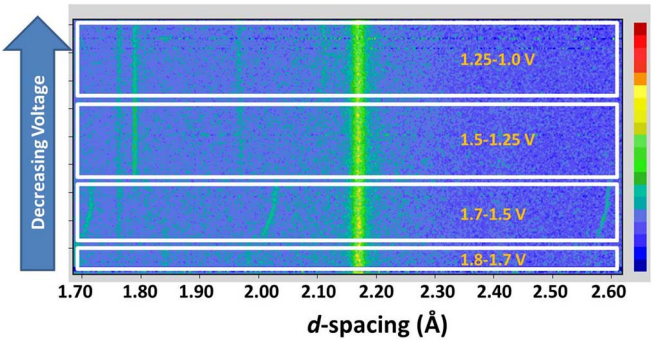

Figure 4. Film plot of powder neutron diffraction data collected upon discharge of a thermal battery using CoS_2 as the cathode. The *y*-axis is not a linear function of voltage, but data-set number.

and these include CoS_2, MgO, KCl, LiCl and LiF. CoS_2 has the pyrite structure, whilst all other phases adopt the rock-salt structure. Several unindexed peaks could be observed in the diffraction pattern, the most prominent at 1.67 Å which could be indexed to a 5.3777(4) Å cubic unit cell, indicating a $LiBr_{1-x}Cl_x$ solid solution and this suggests that halide exchange occurs in the eutectic salt. The unit cell parameters of the phases present at room temperature are given in Table I. No peaks were observed from the $Li_{13}Si_4$ anode, presumably due to the loss in crystallinity during processing and the fact that it adopts a low symmetry structure with a large unit cell.

After room temperature data collection, the cell was heated to a temperature above the melting point of the LiCl-KCl molten salt electrolyte. Once the cell had reached 520°C, the battery was discharged potentiostatically. The resulting powder diffraction data collected during discharge are shown in Figure 4 as a film plot. This indicates four different regions, one region between 1.8 and 1.7 V, a second region between 1.7 and 1.5 V, the third region between 1.5 and 1.25 V and the final region between 1.25 and 1.0 V.

In order to both identify and quantify the phases present upon discharge, Rietveld refinement was carried out. The structured background in the diffraction patterns arising from the amorphous quartz vessel of the Conductivity Rig was modelled using seven diffuse scattering parameters based on the Si-O, Si-Si and O-O interatomic distances in quartz. In addition a further four parameters using a reciprocal linear interpolation function were added to account for the overall decrease in background intensity over the *d*-spacing range used. In the latter stages of the refinements all background parameters were fixed. Cell parameters, phase fractions and peak width parameters were refined for each phase present, but the quality of the data did not allow reliable extraction of atomic thermal vibration parameters and these were fixed during the structure refinement. The low signal to noise ratio in the powder diffraction patterns is due to the relatively thin battery used during the experiment in order to obtain a more realistic electrochemical performance. The separator, MgO, was present in all diffraction patterns. Figures 5a–5d show multiphase Rietveld fits for data collected during the CoS_2 cell discharge, at potentials of 1.6 V, 1.4 V, 1.2 V and 1.1 V. At 1.6 V (Figure 5a), no CoS_2 is present in the diffraction pattern, and only CoS and Li_2S are observed. From Figure 4a clear expansion in the "CoS" unit cell is observed as evidenced by the movement of peaks at *d*-spacings of ∼1.7, ∼2.0 and ∼2.6 Å which could indicate lithium incorporation into this phase or sulfur loss. Due to the relatively fast data collections, the cell parameter evolution in this region cannot be accurately determined; however, the expansion is significant approaching 1% for both *a* and *c* based upon the observed peak shifts. Comparing the unit cell volume per Co atom, Co_9S_8 is about 3.5% larger than CoS, suggesting that CoS loses S to form CoS_{1-y} as its composition moves toward Co_9S_8. Figure 5b shows the diffraction data collected at 1.4 V. The CoS_{1-y} phase is no longer present in the diffraction pattern, indicating that the "CoS_{1-y}" phase has converted to Co_9S_8. At 1.2 V (Figure 5c) Co_9S_8 is still present in the diffraction pattern, but by 1.1 V (Figure 5d), Co is now present in the diffraction pattern. However, at this voltage, the battery discharge is not complete as some Co_9S_8 remains in the diffraction pattern. At this stage the voltage is below the cutoff point for practical applications, so the experiment was stopped. The resulting unit cell parameters for the different crystalline phases present during battery discharge at 520°C are given in Table II.

The phase fractions extracted from the multiple phase Rietveld refinements are plotted in Figures 6a and 6b. Figure 6a shows the phase fraction obtained from Rietveld refinement plotted with the battery discharge profile obtained during the in situ experiment, whilst Figure 6b shows the phase fraction as a function of voltage. Between 1.8 and 1.6 V, the plateau observed in the electrochemical data corresponds to the CoS_2 to CoS + Li_2S transition. A slope then occurs in the battery discharge profile between 1.6 V and 1.4 V and the CoS (via CoS_{1-y}) to Co_9S_8 transformation is responsible for this transition.

Table I. Unit cell parameters for crystalline components of the battery at room temperature before battery discharge.

Phase	Unit Cell Parameters at room temperature(Å)
MgO	4.20843(9)
CoS_2	5.5332(3)
KCl	6.2962(4)
LiCl	5.14194(14)
LiF	4.0287(3)
$LiBr_{1-x}Cl_x$	5.3777(4)

Table II. Unit cell parameters of the crystalline phases present at 520°C.

Phase	Unit Cell Parameters at 520°C (Å)	
MgO	$a = 4.23580(10)$	
Li_2S	$a = 5.7949(7)$	
CoS_2	$a = 5.5713(7)$	
CoS	$a = 3.4162(5)$	$c = 5.3235(14)$
Co_9S_8	$a = 10.0092(9)$	
Co	$a = 3.5669(15)$	

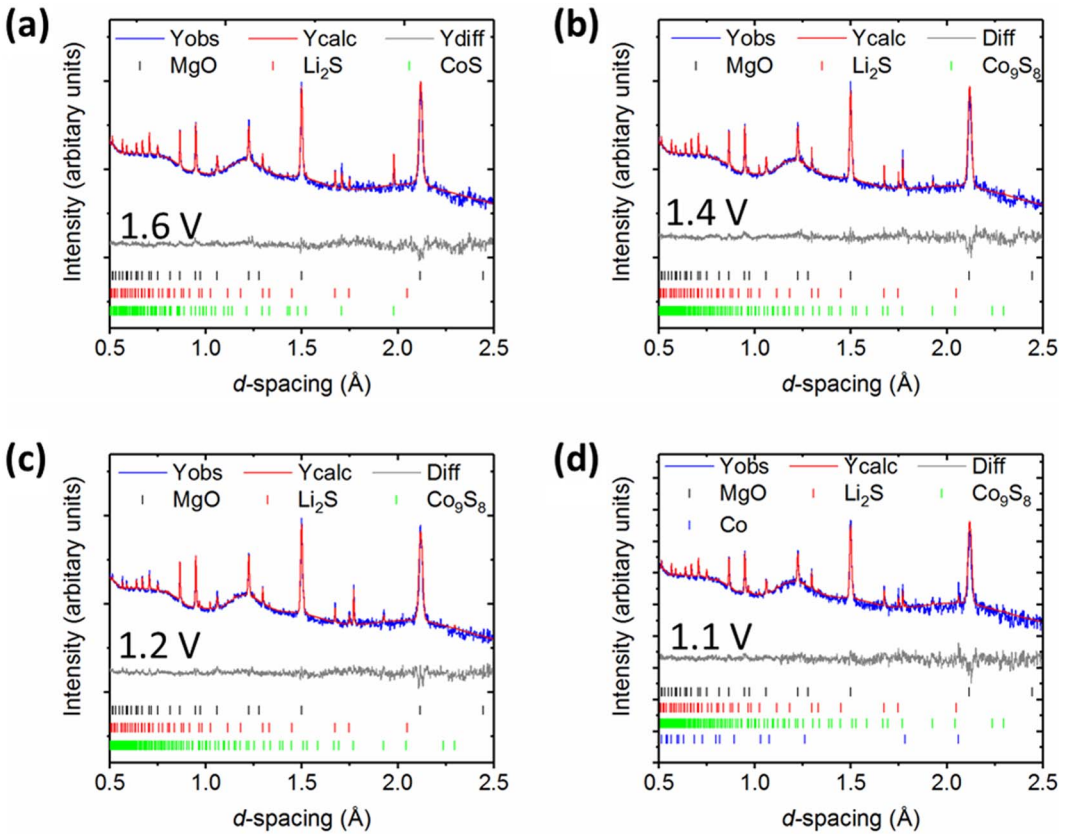

Figure 5. Multiphase Rietveld fits for data collected at voltages of (a) 1.6 V, (b) 1.4 V, (c) 1.2 V, (d) 1.1 V.

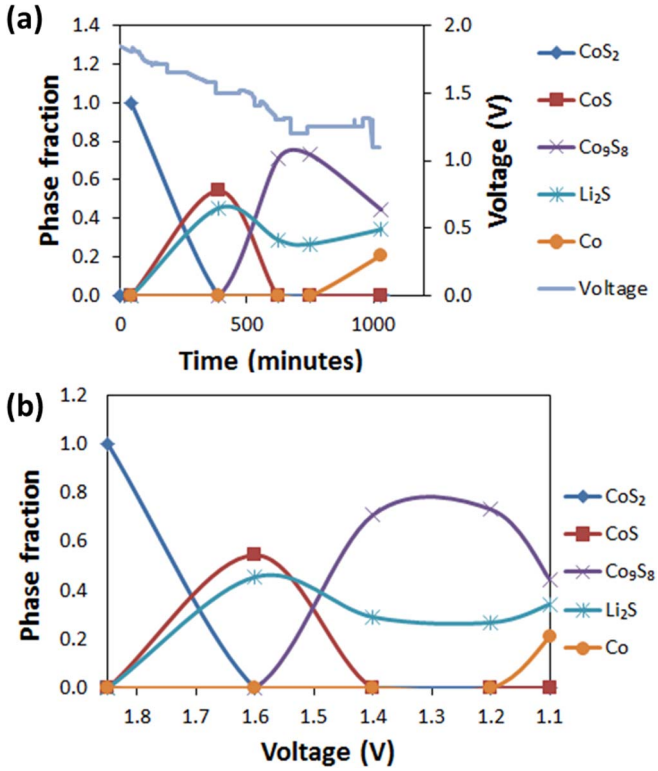

Figure 6. Phase fractions (as weight percent) extracted from multiphase Rietveld refinement (a) Evolution of phase fraction and voltage with time and (b) variation of phase fraction with voltage.

Finally, the transformation of Co_9S_8 to Co accounts for the final plateau, from 1.2 V to 1.1 V.

The discharge mechanism previously outlined by Preto et al. is given in Equation 1:

$$CoS_2 \rightarrow Co_3S_4 + Li_2S \rightarrow Co_9S_8 + Li_2S \rightarrow Co + Li_2S \quad [1]$$

However, during our experiment we see no evidence for the formation of Co_3S_4. Instead, we see the presence of the hexagonal CoS related phase. As can be seen in Figure 4, the cell parameters of the hexagonal CoS phase increase during discharge. The most likely cause for this increase in cell parameter is sulfur loss, as further discharge leads to a cobalt sulfide with lower S content, Co_9S_8. This leads us to propose a new discharge mechanism:

$$CoS_2 + 2\,Li \rightarrow CoS + Li_2S \quad [2]$$

$$CoS + 2/9\,Li \rightarrow 1/9\,Co_9S_8 + 1/9\,Li_2S \quad [3]$$

$$1/9\,Co_9S_8 + 16/9\,Li \rightarrow Co + 8/9\,Li_2S \quad [4]$$

Interestingly, this proposed discharge mechanism also has similarities to the mechanism recently determined during the in situ discharge of a thermal battery using a NiS_2 cathode.[11] In both instances, the first discharge step involves $MS_2 \rightarrow MS$ (M = Co, Ni), which is accompanied by an increase in cell parameter in the MS phase associated with sulfur deficiency. Therefore, our in situ battery discharge experiments carried out at high temperature suggest that there are more similarities in the discharge mechanism for MS_2 (M = Co, Ni) than originally thought, as based on the work of Preto et al.[13] The discharge mechanisms previously proposed by Preto et al. were different, depending on the transition metal present in the cathode.

Conclusions

In this experiment, we have probed the evolution of the crystalline phases upon discharge of a thermal battery employing CoS_2 as a cathode, by collecting neutron powder diffraction data and electrochemical data simultaneously. We have proposed a new discharge mechanism which includes CoS and does not involve the Co_3S_4 spinel phase. There is an increase in cell parameter of the CoS phase during discharge and this warrants more detailed investigation. The most likely reason for this increase in cell parameter is sulfur loss to form lithium sulfide on discharge. The identification of CoS in the discharge mechanism of CoS_2 cathodes is significant as it suggests that the CoS_2 and NiS_2 discharge mechanisms are more similar than originally thought, as both mechanisms have now been shown to include a MS phase (where M = Co or Ni) with the NiAs structure, and in both cases there is an increase in cell parameter.

Acknowledgments

We thank AWE and the EPSRC (EP/K015540/1) for funding. JTSI acknowledges a Royal Society Wolfson Research Merit award. We thank the STFC for beam-time.

ORCID

Julia L. Payne https://orcid.org/0000-0003-3324-6018
Ronald I. Smith https://orcid.org/0000-0002-4990-1307
John T. S. Irvine https://orcid.org/0000-0002-8394-3359

References

1. R. A. Guidotti and P. Masset, *J. Power Sources*, **161**, 1443 (2006).
2. P. Masset and R. A. Guidotti, *J. Power Sources*, **164**, 397 (2007).
3. R. A. Guidotti and P. J. Masset, *J. Power Sources*, **183**, 388 (2008).
4. P. J. Masset and R. A. Guidotti, *J. Power Sources*, **178**, 456 (2008).
5. P. J. Masset and R. A. Guidotti, *J. Power Sources*, **177**, 595 (2008).
6. S. Xie, Y. F. Deng, J. Mei, Z. T. Yang, W. M. Lau, and H. Liu, *Composites Part B-Engineering*, **93**, 203 (2016).
7. R. A. Guidotti, F. W. Reinhardt, J. Dai, and D. E. Reisner, *J. Power Sources*, **160**, 1456 (2006).
8. Y. Wang, J. J. Wu, Y. F. Tang, X. J. Lii, C. Y. Yang, M. S. Qin, F. Q. Huang, X. Li, and X. Zhang, *ACS Appl. Mater. Inter.*, **4**, 4246 (2012).
9. R. C. Jin, J. H. Zhou, Y. S. Guan, H. Liu, and G. Chen, *J. Mater. Chem. A*, **2**, 13241 (2014).
10. Q. H. Wang, L. F. Jiao, Y. Han, H. M. Du, W. X. Peng, Q. N. Huan, D. W. Song, Y. C. Si, Y. J. Wang, and H. T. Yuan, *J. Phys. Chem. C*, **115**, 8300 (2011).
11. J. L. Payne, J. D. Percival, K. Giagloglou, C. J. Crouch, G. M. Carins, R. I. Smith, R. Comrie, R. K. B. Gover, and J. T. S. Irvine, *ChemElectroChem*, **4**, 1 (2017).
12. O. Bergstrom, A. M. Andersson, K. Edstrom, and T. Gustafsson, *J. Appl. Crystallogr.*, **31**, 823 (1998).
13. S. K. Preto, Z. Tomczuk, S. Vonwinbush, and M. F. Roche, *J. Electrochem. Soc.*, **130**, 264 (1983).
14. J. L. Payne, K. Giagloglou, G. M. Carins, C. J. Crouch, J. D. Percival, R. I. Smith, R. K. B. Gover, and J. T. S. Irvine, *Front. Energy Res.*, **6**, 121 (2018).
15. A. C. Larson and R. B. von Dreele, *General Structure Analysis System (GSAS)*, in, Los Alamos National Laboratory Report (2004).
16. B. H. Toby, *J. Appl. Crystallogr.*, **34**, 210 (2001).
17. J. Rodriguez-Carvajal, *Physica B*, **192**, 55 (1993).
18. T. Roisnel and J. Rodriguez-Carvajal, in *EPDIC 7: European Powder Diffraction, Pts 1 and 2*, R. Delhez and E. J. Mittemeijer Editors, p. 118 (2001). *The research data underpinning this publication can be accessed at* https://doi.org/10.17630/d543c2bb-bd53-4688-aec1-83ec38349898.